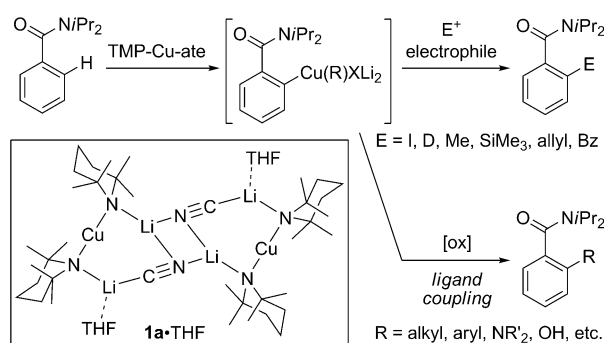


Amidocuprates for Directed *ortho* Cupration: Structural Study, Mechanistic Investigation, and Chemical Requirements**

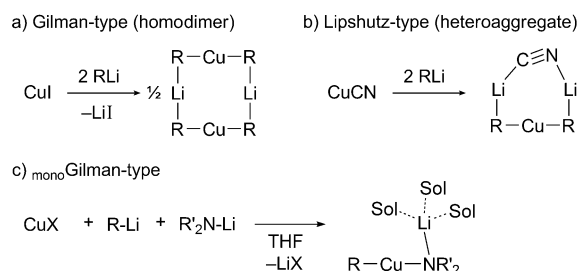
Shinsuke Komagawa,* Shinya Usui, Joanna Haywood, Philip J. Harford, Andrew E. H. Wheatley,* Yotaro Matsumoto, Keiichi Hirano, Ryo Takita, and Masanobu Uchiyama*

Organocuprate(I) complexes are immensely valuable reagents for both industrial and research chemistry.^[1] During the past few decades, heteroleptic organocuprates bearing alkynyl,^[2a,b] cyano,^[2c,d] phenylthio,^[2e] and phosphino^[2f,g] groups have secured an important place in organic synthesis. Organo-amidocuprates also represent an important class of heteroleptic cuprates in organic transformations, especially in stereoselective syntheses.^[3] In this context, we have recently proposed new uses for amidocuprates, TMP-Cu-ates ([RCu(TMP)(CN)Li]; R = alkyl, phenyl, and TMP; TMP = 2,2,6,6-tetramethylpiperidido), which promote the highly chemoselective, directed *ortho* cupration of multifunctionalized aromatic compounds under mild conditions. The aryl cuprate intermediate can be employed not only in the trapping of electrophiles, but also in oxidative ligand coupling to form new C–C bonds with alkyl/aryl groups or to introduce a hydroxy group (Scheme 1).^[4–6]

Organocuprate(I) chemistry is dominated by two structure types: the Gilman-type and the Lipshutz-type.^[7] The basic diorganocuprate(I) unit in each adopts a linear [R–Cu–R] arrangement. Gilman-type species are known to exhibit homodimeric structures (Scheme 2a). Theoretical predictions^[8] of a preference for head-to-tail dimerization of heteroleptic cuprates have been confirmed by the structure of [MesCu(NBn₂)Li] (Mes = mesityl, Bn = benzyl),^[9]



Scheme 1. Directed *ortho* cupration and functionalization, and the dimer structure of $[(\text{TMP})_2\text{Cu}(\text{CN})\text{Li}_2] \cdot \text{THF}$ (**1a**·THF).^[4] Bz = benzoyl.



Scheme 2. Structures of Gilman- and Lipshutz-type cuprates. Sol = solvent (THF).

although monomer formation has been recorded in the presence of a Lewis base.^[10] In contrast, Lipshutz-type reagents exhibit heteroaggregate structures (Scheme 2b).^[2d,11] The reactivity of Lipshutz-type cuprates ($[\text{RCuR}'\text{Li} \cdot \text{LiCN}]$) is frequently higher than that of the corresponding Gilman-type reagents ($[\text{RCuR}'\text{Li}]$).^[12]

To elucidate what types of cuprates are involved in directed *ortho* cupration we have performed detailed mechanistic investigations, including X-ray analysis and a computational study. This led to the emergence of a monomeric Gilman-type structure (Scheme 2c), a related structure to which has been previously revealed,^[5] as the unprecedented, active species for the directed deprotonation.

The starting point of our investigation was the analysis of a bis(amido)cuprate in the solid state to draw comparisons with the known X-ray structure of the product formed from the reaction of CuCN and LiTMP, namely

[*] Dr. S. Komagawa, Dr. S. Usui, Dr. Y. Matsumoto, Dr. K. Hirano, Prof. Dr. R. Takita, Prof. Dr. M. Uchiyama
 Advanced Elements Chemistry Research Team, RIKEN Advanced Science Institute
 2-1 Hirosawa, Wako-shi, Saitama 351-0198 (Japan)
 and
 Graduate School of Pharmaceutical Sciences
 The University of Tokyo
 7-3-1 Hongo, Bunkyo-ku, Tokyo 113-0033 (Japan)
 E-mail: skomagawa@riken.jp
 uchiyama@mol.f.u-tokyo.ac.jp

Dr. J. Haywood, P. J. Harford, Dr. A. E. H. Wheatley
 Department of Chemistry, University of Cambridge
 Lensfield Road, Cambridge, CB2 1EW (UK)
 E-mail: aehw2@cam.ac.uk

[**] We acknowledge financial support from the Daiichi-Sankyo Foundation, Asahi Glass Foundation, Mitsubishi Foundation, and Uehara Memorial Foundation (to M.U.), JSPS Research Fellowships for Young Scientists (to S.K. and S.U.), and the UK EPSRC (to J.H. and P.J.H.). The calculations were performed at the RICC facility at RIKEN. We thank Dr. James V. Morey for his valuable comments.

Supporting information for this article is available on the WWW under <http://dx.doi.org/10.1002/ange.201204923>.

$[(\text{TMP})_2\text{Cu}(\text{CN})\text{Li}_2]\cdot\text{THF}$ (**1a**·THF, Scheme 1).^[4] Thus, LiTMP was added to CuI in a 2:1 ratio in toluene and the precipitated LiI removed. Storage of the resulting solution at 5 °C allowed the isolation of yellow needles. X-ray crystallographic analysis of these revealed the Gilman-type bis(amido)cuprate $[(\text{TMP})_2\text{CuLi}]$ (**1b**), which adopted a centrosymmetric, cyclic dimer structure in the solid state (N1–Cu1 1.926(2), N2–Cu1 1.924(2), N1A–Li1 2.047(4), N2–Li1

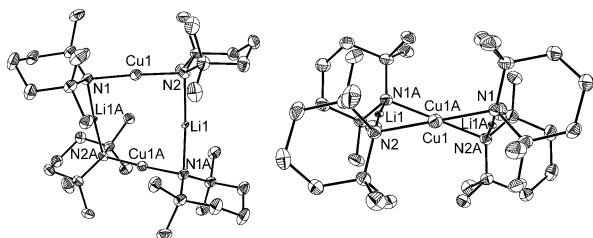


Figure 1. The solid-state dimer of $[(\text{TMP})_2\text{CuLi}]$ (**1b**) plotted at 30% probability. Hydrogen atoms are omitted for clarity. In the right-hand image, Cu1 eclipses Cu1A.

2.075(4) Å; Figure 1). The structure of **1b** was similar to those noted for homoleptic bis(alkyl)- and bis(aryl)cuprates, as well as for heteroleptic $[\text{MesCu}(\text{NBn}_2)\text{Li}]$ (i.e., the Gilman-type structure shown in Scheme 2a),^[9] but it contrasts with those of the TMP-containing cuprates $[\text{RCu}(\mu\text{-TMP})\text{Li}]_n\text{L}$ (R = Ph, $n = 3$, L = THF; R = Me, $n = 1$, L = TMEDA = *N,N,N',N'*-tetramethylethylenediamine), both of which had _{mono} Gilman-type structures (i.e., Scheme 2c, see above).^[5]

Cuprate $[(\text{TMP})_2\text{CuLi}]$ (**1b**) proved to be unreactive for the directed *ortho* cupration of *N,N*-diisopropylbenzamide (**2a**) in THF. Of course, dissolution of the crystalline material may result in changes to the structure and aggregation state. However, the observation that structures of the type exemplified by **1b** can exist in both toluene and THF^[13] is consistent with the fact that the dimer of the unsolvated Gilman-type $[(\text{TMP})_2\text{CuLi}]$ (**1b**) resists THF coordination and is not involved in the directed *ortho* cupration. On the other hand, $[(\text{TMP})_2\text{Cu}(\text{CN})\text{Li}_2]\cdot\text{THF}$ (**1a**·THF), the structure of which was determined to be of the Lipshutz-type^[4] and which exhibited a structural motif akin to that previously noted in bis(aryl)bromocuprates,^[14] reacted smoothly with **2a** to give the product in 85% yield after quenching with I_2 . Furthermore, the fact that the addition of LiCN to **1b** effectively replicated this reaction suggests that LiCN plays a crucial role in breaking up the stable dimer of $[(\text{TMP})_2\text{CuLi}]$ to yield a reactive Lipshutz-type reagent. Indeed, it proved possible to obtain a Lipshutz-type cuprate through exposure of LiTMP to CuI in the presence of THF (in the ratio 2:1:1). This gave a yellow solution that afforded colorless blocks at 5 °C. ¹H NMR spectroscopic analysis of this material revealed the presence of THF and TMP in a 1:2 ratio. Furthermore, elemental analysis indicated that the iodine content was consistent with the Lipshutz-type analogue of **1a**·THF, thus suggesting the formation of bis(amido)cuprate $[(\text{TMP})_2\text{CuLi}_2]\cdot\text{THF}$ (**1c**·THF). X-ray diffraction confirmed a dimeric solid-state structure composed of two crystallographically independent monomers (Figure 2; one represen-

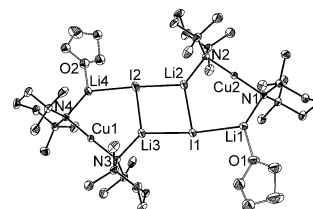
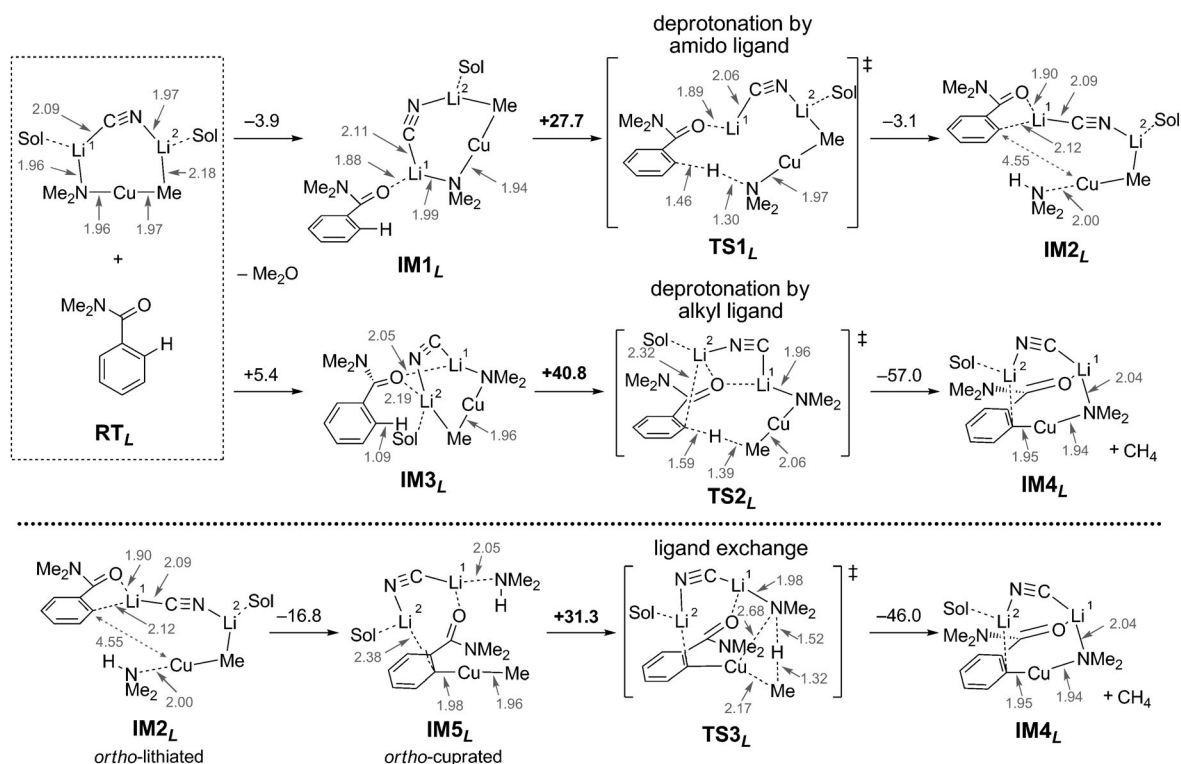


Figure 2. The dimer of $[(\text{TMP})_2\text{CuLi}_2]\cdot\text{THF}$ (**1c**·THF) plotted at 30% probability. Hydrogen atoms and the minor iodide and THF disorder are omitted.

tative monomer is discussed here). The core of (**1c**·THF)₂ incorporates two lithium bis(TMP)cuprate moieties linked through a four-membered (Li)₂ metallocycle. The structure is closely related to that of **1a**·THF, with Cu maintaining a near linear geometry (N(1)–Cu(2)–N(2) 179.77(10)°) and each amide acting as an intermetal bridge (Cu(2)–N(1)–Li(1) 94.13(17), Cu(2)–N(2)–Li(2) 93.11(18)°). Construction of the Lipshutz-type dimer can, therefore, be viewed formally as resulting from the “insertion” of two units of in situ generated LiI·THF into two Li–N bonds of a Gilman-type dimeric ring (see **1b**₂). Thus, we can conclude that in the case of bis(TMP)cuprate, the structural change from Gilman- to Lipshutz-type (i.e., from **1b** to **1c**) is enabled by the presence of both LiI and THF (1 equivalent with respect to Cu). Importantly, the directed *ortho* cupration of **2a** was promoted by the use of in situ generated $[(\text{TMP})_2\text{CuLi}_2]$ (**1c**) to afford the iodinated product in 93% yield after quenching with iodine, as was recently reported in the case of **1a**.^[4,5] Given the similarity between **1a** and **1c** in terms of structure and reactivity, it appears that the generation of a Lipshutz-type cuprate is important for achieving efficient directed *ortho* cupration. Overall, a combination of X-ray crystallography and analysis of the reactivity has shown that 1) the cyclic dimer of the Gilman-type cuprate $[(\text{TMP})_2\text{CuLi}]$ (**1b**) is unreactive in directed *ortho* cupration and 2) not only **1a** and **1c**, but other Lipshutz-type cuprates also exhibit enhanced deprotonative reactivity (see the Supporting Information).^[4,5]

To gain further insight into the reactive cuprate species and the mechanisms by which they react we performed a DFT study on the directed *ortho* cupration of *N,N*-dimethylbenzamide.^[16] A summary of the deprotonation process using a model Lipshutz-type cuprate is shown in Scheme 3. In common with the previously noted reaction pathways for TMP-Zn-ates^[17] and TMP-Al-ates,^[18] two plausible pathways were discovered for the regioselective *ortho* deprotonation: the deprotonation triggered by the amido or alkyl ligand of the Lipshutz-type cuprate. Initially, substrates (**RT**_L) form the relatively stable electrostatic complexes **IM1**_L and **IM3**_L. Transition state **TS1**_L is then attained by an amido ligand promoted deprotonation (**IM1**_L–**TS1**_L–**IM2**_L). Although the activation barrier is slightly high (+27.7 kcal mol^{–1}) relative to that of **IM1**_L, it is still relatively accessible, thus allowing metalated intermediate **IM2**_L to form. The Cu–NMe₂ bond length computed in **TS1**_L is essentially identical to that in **IM1**_L, which suggests that the amido group in **TS1**_L is oriented towards the *ortho* hydrogen position without significant perturbation of the Cu–NMe₂ bond. The other path modeled



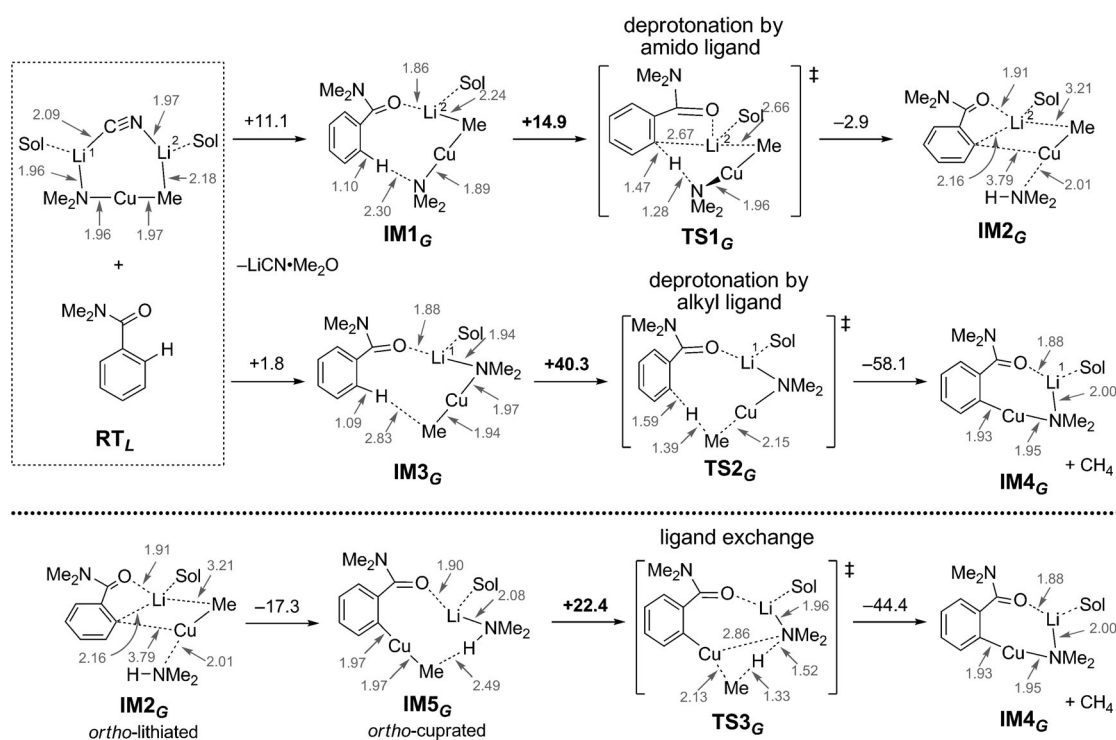
Scheme 3. Modeled pathways for the deprotonation of *N,N*-dimethylbenzamide by [MeCu(NMe₂)(CN)Li₂](OMe₂)₂: deprotonation by the NMe₂ ligand (IM1_L-TS1_L-IM2_L), deprotonation by a Me ligand (IM3_L-TS2_L-IM4_L), and quenching of Me₂NH by a Me ligand (IM5_L-TS3_L-IM4_L). The values are in kcal mol⁻¹, Sol = Me₂O.

involves *ortho* deprotonation by the alkyl component in IM3_L. However, the pathway IM3_L-TS2_L-IM4_L has a high activation energy (+40.8 kcal mol⁻¹ relative to that of IM3_L). Although the formation of IM4_L represents a thermodynamically favorable outcome, the pathway is kinetically unfavorable on account of the relatively high energy of TS2_L. We have also considered the possibility that, subsequent to the *ortho* deprotonation by the amido component, the resultant amine (Me₂NH) could be exchanged with the alkyl ligand on the Cu center to give CH₄ and stable IM4_L (IM5_L-TS3_L-IM4_L). However, the activation barrier to the formation of transition state TS3_L was found to be rather high (+31.3 kcal mol⁻¹ relative to that of IM5_L), thus leading us to conclude that any alkyl-TMP ligand exchange reaction would be slow, or would not proceed at all.

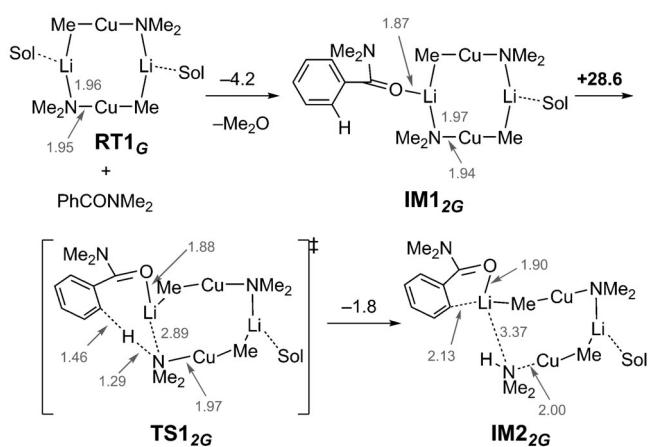
Further investigations into possible pathways for the deprotonation of *N,N*-dimethylbenzamide using the Lipshutz-type reagent led to the identification of an *ortho*-cupration pathway based on the action of the *mono*Gilman-type complex [MeCu(NMe₂)Li]·OMe₂ (Scheme 4). Closely related *mono*Gilman-type species were identified during our previous study,^[5] with one of the solvent molecules coordinated to the lithium ion being substituted by *N,N*-dimethylbenzamide in the complexes IM1_G and IM3_G. Calculations suggest that, by elimination of the solvated LiCN, an initial electrostatic complex (IM1_L) can convert into either of the *mono*Gilman complexes IM1_G or IM3_G, of which the latter is enthalpically preferred by 9.3 kcal mol⁻¹.^[19,20] The pathway IM1_G-TS1_G-IM2_G, in which deprotonation is promoted by the amido

ligand of the *mono*Gilman-type base, has a very low activation barrier (+14.9 kcal mol⁻¹ with respect to that of IM1_G) en route to IM2_G. Although the total activation energy (26.0 kcal mol⁻¹) from RT_L to TS1_G is comparable to that (23.8 kcal mol⁻¹) from RT_L to TS1_L, the *mono*Gilman pathway does not need more than 15 kcal mol⁻¹ in energy for any given step, and this contrasts with the Lipshutz path, which requires over 27 kcal mol⁻¹ for the deprotonation step. A Li⁺ ion assists the *mono*Gilman deprotonation and the formation of IM2_G through its proximity to the aromatic *ortho* position in TS1_G. Although IM3_G is more stable than IM1_G, it fails to promote the deprotonation (IM3_G-TS2_G-IM4_G), a process that reveals a very high activation energy (+40.3 kcal mol⁻¹). As with the Lipshutz system, although quenching of the amine (Me₂NH, IM5_G-TS3_G-IM4_G) was felt unlikely to proceed on account of the rather high energy difference between RT_L and TS3_G (more than 28 kcal mol⁻¹), the activation barrier to reach the transition state TS3_G is entropically permissible at 22.4 kcal mol⁻¹.^[21] Lastly, we also calculated the directed *ortho* cupration pathway starting with the Gilman dimer RT1_G (cf. 1b₂, which is inert for directed *ortho* cupration, Scheme 5). The significant increase in the activation energy of deprotonation by the amido ligand (+28.6 kcal mol⁻¹) is in good agreement with experimental results.^[4,5]

In conclusion, this study has revealed the structures of new TMP-Cu-ates and the possible pathways for directed *ortho* cupration. Both Gilman- and Lipshutz-type crystal structures were found, depending on the preparative con-



Scheme 4. Modeled pathways for the deprotonation by $[\text{MeCu}(\text{NMe}_2)\text{Li}]\cdot\text{OMe}_2$: deprotonation by the NMe_2 ligand (IM1_G - TS1_G - IM2_G), deprotonation by a Me ligand (IM3_G - TS2_G - IM4_G), and ligand exchange with the resultant Me_2NH by a Me ligand (IM5_G - TS3_G - IM4_G). The values are in kcal mol^{-1} , $\text{Sol} = \text{Me}_2\text{O}$.



Scheme 5. Modeled pathways for the deprotonation of *N,N*-dimethylbenzamide by Gilman-type cuprate $[\{\text{MeCu}(\text{NMe}_2)\text{Li}\}_2]\cdot(\text{OMe}_2)_2$. The values are in kcal mol^{-1} , $\text{Sol} = \text{Me}_2\text{O}$.

ditions, with analogous active Lipshutz cuprates being formed in the presence of LiCN or LiI in THF. Theoretical mechanistic investigations indicated that a monomeric Gilman-type alkyl(amido)cuprate (Scheme 2c), generated from a Lipshutz-type precursor rather than from the dimeric Gilman-type substrate, is likely to be the active species in directed *ortho* cupration. The *ortho* deprotonation involves the action of the amido ligand, with the alkyl ligand retained by the aryl cuprate intermediate without further ligand exchange.^[16c] This means that the intermediates (i.e. aryl

cuprate species) of directed *ortho* cupration can easily be used to introduce a variety of functional groups at the aromatic *ortho* position, not only by electrophilic trapping, but also by oxidative functionalization, thanks to the flexible oxidation state of the copper center (Scheme 1).^[4] With the comprehensive mechanistic knowledge acquired here, we are currently improving the reaction scope and logically designing new chemoselective reagents.

Received: June 23, 2012

Revised: September 10, 2012

Published online: October 18, 2012

Keywords: cuprates · density functional calculations · mechanistic studies · *ortho* metalation · structure elucidation

- [1] a) *Modern Organocopper Chemistry* (Ed.: N. Krause), Wiley-VCH, Weinheim, **2002**; b) E. Nakamura, S. Mori, *Angew. Chem.* **2000**, *112*, 3902–3924; *Angew. Chem. Int. Ed.* **2000**, *39*, 3750–3771; c) R. M. Gschwind, *Chem. Rev.* **2008**, *108*, 3029–3053; d) N. Yoshikai, E. Nakamura, *Chem. Rev.* **2012**, *112*, 2339–2372.
[2] a) H. O. House, M. J. Umen, *Org. Chem.* **1973**, *38*, 3893–3901; b) W. H. Mandeville, G. M. Whitesides, *J. Org. Chem.* **1974**, *39*, 400–405; c) J. P. Gorlier, L. Hamon, J. Levisalles, J. Wagnon, *J. Chem. Soc. Chem. Commun.* **1973**, 88a; d) B. H. Lipshutz, R. S. Wilhelm, J. A. Kozlowski, *Tetrahedron* **1984**, *40*, 5005–5038; e) G. H. Posner, C. E. Whitten, J. Sterling, *J. Am. Chem. Soc.* **1973**, *95*, 7788–7797; f) S. H. Bertz, G. Dabbagh, G. M. Villacorta, *J. Am. Chem. Soc.* **1982**, *104*, 5824–5826; g) P. J. Harford, J. Hayward, M. R. Smith, B. N. Bhawal, P. R. Raithby, M.

- Uchiyama, A. E. H. Wheatley, *Dalton Trans.* **2012**, *41*, 6148–6154.
- [3] a) B. E. Rossiter, N. M. Swingle, *Chem. Rev.* **1992**, *92*, 771–806; b) N. Krause, A. Gerold, *Angew. Chem.* **1997**, *109*, 194–213; *Angew. Chem. Int. Ed. Engl.* **1997**, *36*, 186–204; c) R. K. Dieter, in *Modern Organocopper Chemistry* (Ed.: N. Krause), Wiley-VCH, Weinheim, **2002**, pp. 79–144.
- [4] S. Usui, Y. Hashimoto, J. V. Morey, A. E. H. Wheatley, M. Uchiyama, *J. Am. Chem. Soc.* **2007**, *129*, 15102–15103.
- [5] J. Haywood, J. V. Morey, A. E. H. Wheatley, C.-Y. Liu, S. Yasuike, J. Kurita, M. Uchiyama, P. R. Raithby, *Organometallics* **2009**, *28*, 38–41. Herein, “*mono*-Gilman-type” cuprates are also referred to as “Gilman-type” species.
- [6] Very recently, a similar directed *ortho* cupration was reported, see T. T. Nguyen, N. Marquise, F. Chevallier, F. Mongin, *Chem. Eur. J.* **2011**, *17*, 10405–10416.
- [7] R. P. Davies, *Coord. Chem. Rev.* **2011**, *255*, 1226–1251.
- [8] a) R. K. Dieter, M. Tokles, *J. Am. Chem. Soc.* **1987**, *109*, 2040–2046; b) R. K. Dieter, T. W. Hanks, *Organometallics* **1992**, *11*, 3549–3554; c) B. E. Rossiter, M. Eguchi, G. Miao, N. M. Swingle, A. E. Hernandez, D. Vickers, E. Fluckiger, R. G. Patterson, K. V. Reddy, *Tetrahedron* **1993**, *49*, 965–986.
- [9] R. P. Davies, S. Hornauer, P. B. Hitchcock, *Angew. Chem.* **2007**, *119*, 5283–5286; *Angew. Chem. Int. Ed.* **2007**, *46*, 5191–5194.
- [10] R. Bomparola, R. P. Davies, S. Hornauer, J. P. White, *Dalton Trans.* **2009**, 1104–1106.
- [11] a) B. H. Lipshutz, R. S. Wilhelm, D. M. Floyd, *J. Am. Chem. Soc.* **1981**, *103*, 7672–7674; b) B. H. Lipshutz, J. A. Kozlowski, R. S. Wilhelm, *J. Org. Chem.* **1984**, *49*, 3943–3949; c) B. H. Lipshutz, *Synthesis* **1987**, 325–341; d) B. H. Lipshutz, S. Sharma, E. L. Ellsworth, *J. Am. Chem. Soc.* **1990**, *112*, 4032–4034.
- [12] a) B. H. Lipshutz, R. S. Wilhelm, J. A. Kozlowski, *Tetrahedron* **1984**, *40*, 3943–3945; b) B. H. Lipshutz, J. A. Kozlowski, C. M. Breneman, *J. Am. Chem. Soc.* **1985**, *107*, 3197–3204.
- [13] W. Henze, A. Vyater, N. Krause, R. M. Gschwind, *J. Am. Chem. Soc.* **2005**, *127*, 17335–17342.
- [14] a) C. M. P. Kronenburg, J. T. B. H. Jastrzebski, A. L. Spek, G. van Koten, *J. Am. Chem. Soc.* **1998**, *120*, 9688–9689; b) C. M. P. Kronenburg, J. T. B. H. Jastrzebski, J. Boersma, M. Lutz, A. L. Spek, G. van Koten, *J. Am. Chem. Soc.* **2002**, *124*, 11675–11683.
- [15] In Ref. [4], **1c** was reported not to promote the directed *ortho* cupration of benzonitrile. The cylindrical symmetry of the cyano group prevents directed *ortho* cupration, for example, even by alkyl lithium reagents. For the directed *ortho* cupration of benzonitrile, appropriate reagents (e.g. **1a**) are necessary.
- [16] The calculations were performed at the B3LYP/631SVP level of theory. Ahlrich’s SVP all-electron basis set was employed for the Cu atom and 6-31 + G* for other atoms (denoted as 631SVP). Energy changes (ΔG) are shown in kcal mol⁻¹. All calculations were carried with the Gaussian03 program package: M. J. Frisch, et al. Gaussian03, revision E.01; Gaussian, Inc.: Wallingford, CT, **2004**. Details are in the Supporting Information.
- [17] a) Y. Kondo, M. Shilai, M. Uchiyama, T. Sakamoto, *J. Am. Chem. Soc.* **1999**, *121*, 3539–3540; b) M. Uchiyama, T. Miyoshi, Y. Kajihara, T. Sakamoto, Y. Otani, T. Ohwada, Y. Kondo, *J. Am. Chem. Soc.* **2002**, *124*, 8514–8515; c) M. Uchiyama, Y. Matsumoto, D. Nobuto, T. Furuyama, K. Yamguchi, K. Morokuma, *J. Am. Chem. Soc.* **2006**, *128*, 8748–8750; d) M. Uchiyama, Y. Matsumoto, S. Usui, Y. Hashimoto, K. Morokuma, *Angew. Chem.* **2007**, *119*, 944–947; *Angew. Chem. Int. Ed.* **2007**, *46*, 926–929; e) Y. Kondo, J. V. Morey, J. C. Morgan, H. Naka, D. Nobuto, P. R. Raithby, M. Uchiyama, A. E. H. Wheatley, *J. Am. Chem. Soc.* **2007**, *129*, 12734–12738.
- [18] a) M. Uchiyama, H. Naka, Y. Matsumoto, T. Ohwada, *J. Am. Chem. Soc.* **2004**, *126*, 10526–10527; b) H. Naka, M. Uchiyama, Y. Matsumoto, A. E. H. Wheatley, M. McPartlin, J. V. Morey, Y. Kondo, *J. Am. Chem. Soc.* **2007**, *129*, 1921–1930; c) H. Naka, J. V. Morey, J. Haywood, D. J. Eisler, M. McPartlin, F. García, H. Kudo, Y. Kondo, M. Uchiyama, A. E. H. Wheatley, *J. Am. Chem. Soc.* **2008**, *130*, 16193–16920.
- [19] **IM1_G** and **IM3_G** should be generated from **IM1_L** and excess amounts of ethereal solvents, and the direct interconversion of **IM1_G** and **IM3_G** would be hindered due to the difficulty of breaking bonds between the metal centers and the coordinating NMe₂ and Me groups.
- [20] In *mono*-Gilman species with three coordinated THF solvent molecules or one tmeda ligand (Ref. [5]), it was noteworthy that Li was coordinated to N, but no alkyl–lithium interaction was observed due to the linear geometry around the Cu center (N–Cu–C). In **IM1_G** and **IM3_G**, it is reasonable that the intramolecular coordination of *N,N*-dimethylbenzamide through both O_{amide} and H_{ortho} compensate for this.
- [21] The activation energy (ΔE^\ddagger) to **TS3_G** is 31.1 kcal mol⁻¹ at the MP2/631SVP//B3LYP/631SVP level of theory.